

---

# AutoGEL: An Automated Graph Neural Network with Explicit Link Information

---

Zhili WANG, Shimin DI\*, Lei CHEN

Department of Computer Science and Engineering  
The Hong Kong University of Science and Technology  
{zwangeo,sdiaa,leichen}@connect.ust.hk

## Abstract

Recently, Graph Neural Networks (GNNs) have gained popularity in a variety of real-world scenarios. Despite the great success, the architecture design of GNNs heavily relies on manual labor. Thus, automated graph neural network (AutoGNN) has attracted interest and attention from the research community, which makes significant performance improvements in recent years. However, existing AutoGNN works mainly adopt an implicit way to model and leverage the link information in the graphs, which is not well regularized to the link prediction task on graphs, and limits the performance of AutoGNN for other graph tasks. In this paper, we present a novel AutoGNN work that explicitly models the link information, abbreviated to AutoGEL. In such a way, AutoGEL can handle the link prediction task and improve the performance of AutoGNNs on the node classification and graph classification task. Specifically, AutoGEL proposes a novel search space containing various design dimensions at both intra-layer and inter-layer designs and adopts a more robust differentiable search algorithm to further improve efficiency and effectiveness. Experimental results on benchmark data sets demonstrate the superiority of AutoGEL on several tasks.

## 1 Introduction

As one of ubiquitous data structures, graph  $G(E, V)$  contains the node-set  $V = \{v_1, \dots, v_n\}$  and edge-set  $E = \{e(v_i, v_j) : v_i, v_j \in V\}$ , which can represent a lot of real-world data sets, such as social networks [Bu et al., 2018], physical systems [Sanchez-Gonzalez et al., 2018], protein-protein interaction networks [Yue et al., 2020]. In recent years, Graph Neural Networks (GNNs) have been introduced for various graph tasks and achieve unprecedented success, such as node classification [Kipf and Welling, 2016a, Hamilton et al., 2017], link prediction [Vashishth et al., 2019, Li et al., 2020], and graph classification [Niepert et al., 2016, Zhang et al., 2018]. Generally, GNNs encode  $G(V, E)$  into the  $d$ -dimensional vector space (e.g.,  $\mathbf{V} \in \mathbb{R}^{|V| \times d}$ ) that preserves similarity in the original graph. Despite the great success, those GNNs are restricted to specific instances within GNN design space [You et al., 2020]. Different graph tasks usually require different GNN architectures [Gilmer et al., 2017]. For example, compared with the node classification task, GNNs for graph classification introduces an extra readout phase to obtain graph embeddings. However, architecture design for these GNNs remains a challenging problem due to the diversity of graph data sets. Given a graph task, a GNN architecture performs well on one data set does not necessarily imply that it is also suitable for other data sets [You et al., 2020].

Some pioneer works have been proposed to alleviate the above issue in GNN models. They introduce Neural Architecture Search (NAS) [Elsken et al., 2019] approaches to automatically design suitable

---

\*Corresponding author

GNN architecture for the given data set (i.e., AutoGNN) [Zhou et al., 2019, Gao et al., 2020, Jiang and Balaprakash, 2020, Zhao et al., 2021]. Architectures identified by these AutoGNNs rival or surpass the best handcrafted GNN models, demonstrating the potential of AutoGNN towards better GNN architecture design. Unfortunately, the existing AutoGNNs are mainly designed for the node classification and graph classification task. Their designs do not include edge embeddings, i.e., modeling and organizing link information in an implicit way. First, it is difficult for existing AutoGNNs to handle another important graph task on the edge-level, link prediction (LP) task. Second, lack of edge embedding makes them inexpressive to leverage the complex link information, such as direction information of edges and different edge types in multi-relational graphs. Especially, various edge types could impose different influence for encoding nodes into embeddings, which can further improve the model performance on the node-level and graph-level tasks. Therefore, a new AutoGNN is desired to model link information explicitly on various data sets.

To bridge the aforementioned research gap, we propose AutoGEL, a novel *AutoGNN* framework with *Explicit Link* information, which can handle the LP task and improve performance of AutoGNNs on other graph tasks. Specifically, AutoGEL explicitly learns the edge embedding in the message passing framework to model the complex link information, and introduces the several novel design dimensions into the GNN search space, enabling a more powerful GNN to be searched for any given graph data set. Moreover, AutoGEL adopts a robust differentiable search algorithm to guarantee the effectiveness of searched architectures and control the computational footprint. We summarize the contributions of this work as follows:

- The design of existing AutoGNNs follows an implicit way to leverage and organize the link information, which cannot handle the LP task and limits the performance of AutoGNNs on other graph tasks. In this paper, we present a novel method called AutoGEL to solve these issues through explicitly modeling the link information in the graphs.
- AutoGEL introduces several novel design dimensions into the GNN search space at both the intra-layer and inter-layer designs, so as to improve the task performance. Moreover, motivated by one robust NAS algorithm SNAS, AutoGEL upgrades the search algorithm adopted in existing AutoGNNs to further guarantee the effectiveness of final derived GNN.
- The experimental results demonstrate that AutoGEL can achieve better performance than manually designed models in the LP task. Furthermore, AutoGEL shows excellent competitiveness with other AutoGNN works on the node and graph classification tasks.

## 2 Related Work

### 2.1 General Message Passing Framework

The majority of GNNs follow the neighborhood aggregation schema [Gilmer et al., 2017], i.e., the Message Passing Neural Network (MPNN), which is formulated as:

$$\mathbf{m}_v^{k+1} = AGG_k(\{M_k(\mathbf{h}_v^k, \mathbf{h}_u^k, \mathbf{e}_{vu}^k) : u \in N(v)\}), \mathbf{h}_v^{k+1} = ACT_k(COM_k(\{\mathbf{h}_v^k, \mathbf{m}_v^{k+1}\})), \quad (1)$$

$$\hat{\mathbf{y}} = R(\{\mathbf{h}_v^L | v \in G\}), \quad (2)$$

where  $k$  denotes  $k$ -th layer,  $N(v)$  denotes a set of neighboring nodes of  $v$ ,  $\mathbf{h}_v^k$ ,  $\mathbf{h}_u^k$  denotes hidden embeddings for  $v$  and  $u$  respectively,  $\mathbf{e}_{vu}^k$  denotes features for edge  $e(v, u)$  (optional),  $\mathbf{m}_v^{k+1}$  denotes the intermediate embeddings gathered from neighborhood  $N(v)$ ,  $M_k$  denotes the message function,  $AGG_k$  denotes the neighborhood aggregation function,  $COM_k$  denotes the combination function between intermediate embeddings and embeddings of node  $v$  itself from the last layer,  $ACT_k$  denotes activation function. Such message passing phase in (1) repeats for  $L$  times (i.e.,  $k \in \{1, \dots, L\}$ ). For graph-level tasks, it further follows the readout phase in (2) where information from the entire graph  $G$  is aggregated through readout function  $R(\cdot)$ .

### 2.2 Automated Graph Neural Networks (AutoGNN)

In recent years, AutoGNN has emerged as a promising direction towards better graph neural architecture design [Zhou et al., 2019, Gao et al., 2020, Jiang and Balaprakash, 2020, You et al., 2020, Zhao et al., 2021, Ding et al., 2021]. To enable a powerful GNN architecture to be searched, AutoGNNs first propose the GNN search space in the *intra-layer* level, i.e., providing common choices for several

Table 1: Overview of Existing AutoGNN Works. The ‘‘Differ.’’ denotes to differentiable algorithm.

Method	Graph	MPNN Space		Search Algorithm	Task	
	#node/edge types	$\mathbf{h}_e$	intra inter			
GraphNAS	$\geq 1/ = 1$	$\times$	$\checkmark$	$\times$	RL	node
AGNN	$\geq 1/ = 1$	$\times$	$\checkmark$	$\times$	EA+RL	node
SANE	$\geq 1/ \geq 1$	$\times$	$\checkmark$	$layer\_cnt \& \_agg$	deterministic Differ.	node
NAS-GCN	$\geq 1/ \geq 1$	$\times$	$\checkmark$	$layer\_cnt$	EA	graph
You et al. [2020]	$\geq 1/ = 1$	$\times$	$\checkmark$	$layer\_cnt$	random	node/edge/graph
AutoGEL	$\geq 1/ \geq 1$	$\checkmark$	$\checkmark$	$layer\_cnt \& \_agg$	stochastic Differ.	node/edge/graph

important operators in one MPNN layer (see (1) and (2)). Here we summarize candidate choices for those operators:

- **Message Function**  $M_k$ : Existing AutoGNNs mainly focus on the node-level and graph-level task, thus edge embeddings are often not available.  $M_k(\mathbf{h}_v, \mathbf{h}_u, \mathbf{e}_{vu})$  is reduced to  $M_k(\mathbf{h}_v, \mathbf{h}_u)$ . Typically,  $M(\mathbf{h}_v, \mathbf{h}_u) = a_{vu} \mathbf{W} \mathbf{h}_u$ , where  $a_{vu}$  denotes the attention scores, and  $\mathbf{W} \in \mathbb{R}^{d \times d}$  denotes the linear transformation matrix. Note that NAS-GCN [Jiang and Balaprakash, 2020] only takes the edge feature  $\mathbf{e}_{vu}$  as input without learning edge embeddings. We next denote the edge embedding to  $\mathbf{h}_e$  for distinguishing.
- **Aggregation**  $AGG_k$ : It controls the way to aggregate message from nodes’ neighborhood. It can be any differentiable and permutation invariant functions, usually  $AGG_k \in [sum, mean, max]$ . And  $sum(\cdot) = \sum_{u \in N(v)} M_k(\mathbf{h}_v, \mathbf{h}_u)$ ,  $mean(\cdot) = \sum_{u \in N(v)} M_k(\mathbf{h}_v, \mathbf{h}_u) / |N(v)|$ , and  $max(\cdot)$  denotes channel-wise maximum across the node dimension.
- **Combination**  $COM_k$ : It determines the way to merge messages between neighborhood and node itself. In literature,  $COM_k$  is selected from  $[concat, add, mlp]$ , where  $concat(\cdot) = [\mathbf{h}_v^k, \mathbf{m}_v^{k+1}]$ ,  $add(\cdot) = \mathbf{h}_v^k + \mathbf{m}_v^{k+1}$ , and  $mlp(\cdot) = \text{MLP}(\mathbf{h}_v^k + \mathbf{m}_v^{k+1})$  (MLP is Multi-layer Perceptron).
- **Activation**  $ACT_k$ :  $[identity, sigmoid, tanh, relu, elu]$  are some of the most commonly used activation functions [Gao et al., 2020].
- **Graph Pooling**: The pooling operator has been introduced for the graph classification task, such as  $[global\ pool, global\ attention\ pool, flatten]$  [Jiang and Balaprakash, 2020, Wei et al., 2021].

In addition to the above intra-layer operators, several works [You et al., 2020, Zhao et al., 2021, Jiang and Balaprakash, 2020] propose the idea of searching layer connectivity to combine hidden representations of different layers in a better way, i.e., *inter-layer* design. More details will be discussed in Sec. 3.1.2. After the search space design, AutoGNNs adopt various search algorithms to search the optimal architecture from the search space. AGNN [Zhou et al., 2019] and GraphNAS [Gao et al., 2020] follow the reinforcement learning (RL) [Williams, 1992] way to search architectures. They utilize a recurrent neural network controller for architecture sampling, and update the controller to maximize the expected performance of sampled architectures. NAS-GCN [Jiang and Balaprakash, 2020] adopt evolutionary algorithm (EA), where new architectures are generated by performing mutation from parent architectures and the population, i.e., the best performing architectures, are iteratively updated. However, both RL and EA algorithms require a large number of architectures to be sampled, which is inherently computational expensive. To improve the search efficiency, SANE [Zhao et al., 2021] adopts a deterministic differentiable search algorithm DARTS [Liu et al., 2018], where a supernet containing all candidate operators is constructed and architecture parameters are jointly optimized with network parameters through gradient descent. Unfortunately, it has been discussed in SNAS [Xie et al., 2018] that DARTS suffer from the unbounded bias issue towards its objective, which limits the performance of the final derived model. In Tab. 1, we summarize existing AutoGNNs from several perspectives: graph, MPNN space, search algorithm, and task scenario.

### 2.3 GNNs for Link Prediction Task

Even with the great effort invested into the construction and maintenance of networks, many graph data sets still remain incomplete [Schlichtkrull et al., 2018]. Therefore, the link prediction (LP) task is one of the most crucial problems in the graph-structured data, which aims to recover those

missing links in a graph [Zhang et al., 2019, 2020a], i.e., predicting the missing node in  $e(v_i, ?)$  where  $?$  denotes the target node that has the potential link with  $v_i$ . Recently, GNN models have been introduced to handle the LP task (abbreviated to GLP models), which can be roughly categorized based on its application scenarios: GLP on homogeneous graphs (i.e., only one type of nodes and edges [Yang et al., 2016]), and multi-relational graphs (i.e., graphs with multiple edge types [Toutanova and Chen, 2015]).

### 2.3.1 Link Prediction on Homogeneous Graphs

As one of the classic approaches for LP task on such homogeneous graphs, heuristic methods predict link existence according to heuristic node similarity scores [Zhang et al., 2020b]. Despite its effectiveness in some scenarios, heuristic methods hold strong assumptions on the link formation mechanism, i.e., highly similar nodes have links. It would fail on those networks where their assumptions do not hold [Zhang and Chen, 2018]. Furthermore, latent feature-based methods [Perozzi et al., 2014, Grover and Leskovec, 2016] factorize some network matrices to learn node embeddings in a transductive way, which limits their generalization ability to unseen data.

Recently, several GLP models have been proposed for the LP task on homogeneous graphs. GAE [Kipf and Welling, 2016b] applies GNN model over the entire graph and aims to learn node embeddings that minimize the graph reconstruction cost through:

$$\mathbf{H} = GCN(\mathbf{X}, \mathbf{A}), \hat{\mathbf{A}} = \sigma(\mathbf{H}\mathbf{H}^\top) \quad (3)$$

where  $\mathbf{X} \in \mathbb{R}^{|V| \times D}$  is the feature matrix of nodes,  $\mathbf{A} \in \mathbb{R}^{|V| \times |V|}$  is the adjacency matrix,  $\mathbf{H}$  is the learned node representations,  $\sigma(\cdot)$  is the logistic sigmoid function,  $\hat{\mathbf{A}}$  denotes the reconstructed adjacency matrix, whose entry  $\hat{A}_{uv}$  is the predicted score (between 0-1) for target link  $e_{uv}$ . However, GAE focus on aggregating node attributes only.

SEAL [Zhang and Chen, 2018] and DE-GNN [Li et al., 2020] propose to learn the link embedding from the subgraph structures. Specifically, DE-GNN [Li et al., 2020] considers feature of subgraph structure  $\mathbf{X}^{sub}$  for aggregation and utilize node-set level readout:

$$\mathbf{H}^{sub} = GCN(\mathbf{X}^{sub}, \mathbf{A}^{sub}), \mathbf{h}_e = R(\{\mathbf{h}_v | v \in S\}), \quad (4)$$

where  $S = \{u, v\}$  denotes two nodes in the link  $e(u, v)$  for LP task, and  $R(\cdot)$  is difference-pooling in DE-GNN, i.e.,  $R(\cdot) = |\mathbf{h}_u - \mathbf{h}_v|$ .

### 2.3.2 Link Prediction on Multi-relational Graphs

Different from graph form  $G(E, V)$ , the multi-relational graph  $G(E, V, R)$  usually contains different types of edges, where  $r(u, v)$  indicates the edge type  $r \in R$  existing between  $u$  and  $v$ . For example, in recommendation system, users and items are nodes of the bipartite graph, and the edge between nodes could be “click” and “add\_to\_cart”. In the knowledge graph (KG) scenario, nodes represent real-world entities and edges are relations between entities.

Recently, several GLP models have been developed for the LP task on KGs [Schlichtkrull et al., 2018, Vashishth et al., 2019]. Based on the MPNN framework in (1) and (2), R-GCN [Schlichtkrull et al., 2018] proposes to model different edge types through edge-specific weight matrix  $\mathbf{W}_r^k$  for  $r \in R$ , where the MPNN in R-GCN is instantiated as:

$$\mathbf{h}_v^{k+1} = ACT_k \left( \sum_{r(u,v)} \mathbf{W}_r^{k+1} \mathbf{h}_u^k \right) \quad (5)$$

Similar to R-GCN modeling, D-GCN [Marcheggiani and Titov, 2017] and W-GCN [Shang et al., 2019] are also restricted to learning embeddings for nodes only. Instead, CompGCN [Vashishth et al., 2019] propose to jointly learn entity and relation embeddings:

$$\mathbf{h}_v^{k+1} = ACT_k \left( \sum_{r(u,v)} \mathbf{W}_{\lambda(r)}^{k+1} \phi(\mathbf{h}_u^k, \mathbf{h}_r^k) \right) \quad (6)$$

where  $\mathbf{h}_r^k$  denotes the embedding vector for the specific edge type  $r$ , and  $\lambda(r) \in [incoming, outgoing, self\_loop]$  records information of directed edges.  $\phi : \mathbb{R}^d \times \mathbb{R}^d \rightarrow \mathbb{R}^d$  can be any entity-relation composition operation, such as *sub* in TransE [Bordes et al., 2013].

Compared with earlier approaches, GLP models bring remarkable performance gains, illustrating their superiority over LP task. However, exiting GLP models rely on manual and empirical graph neural architecture design, such as selecting proper  $ACT(\cdot)$  and  $\phi(\cdot)$ . Thus, a data-aware GLP model is desired.

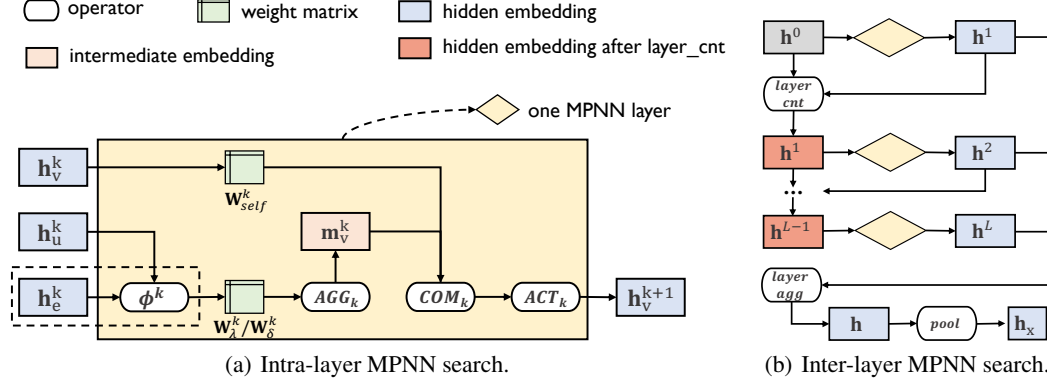


Figure 1: The illustration to AutoGEL’s search space: a) given representation  $\mathbf{h}^k$  in  $k$ -th layer (including edge embedding  $\mathbf{h}_e^k$  if available), AutoGEL searches for proper operators of  $\phi^k$ ,  $\mathbf{W}^k$ ,  $AGG_k$ ,  $COM_k$ ,  $ACT_k$  in the intra-layer space, then outputs the hidden node representation  $\mathbf{h}_v^{k+1}$ . Note that the dotted area will be activated in the scenario of multi-relational graphs.

### 3 AutoGEL: AutoGNN with Explicit Link Information

#### 3.1 Search Space

In this subsection, AutoGEL explicitly models the link information in the MPNN space, and proposes several novel operators at both intra-layer (i.e., the message passing in a specific layer) and inter-layer designs (i.e., the message passing across layers). The overflow of space is shown in Fig. 1.

##### 3.1.1 Intra-layer Message Passing Design

As discussed in Sec. 1 and Sec. 2.2, existing AutoGNNs lack modeling of links, which only utilize the pure link information of the node neighborhood. Such implicit way fails to handle and leverage the complex link information. To solve this issue, we present a novel intra-layer message passing framework, which instantiates (1) as:

$$\mathbf{m}_v^{k+1} = AGG_k(\{\mathbf{W}_{\delta(u)}^k \mathbf{h}_u^k : u \in N(v)\}), \quad (7)$$

$$\mathbf{m}_v^{k+1} = AGG_k(\{\mathbf{W}_{\lambda(e)}^k \phi^k(\mathbf{h}_u^k, \mathbf{h}_e^k) : u \in N(v)\}), \quad (8)$$

$$\mathbf{h}_v^{k+1} = ACT_k(COM_k(\{\mathbf{W}_{self}^k \mathbf{h}_v^k, \mathbf{m}_v^{k+1}\})), \quad (9)$$

where (7) and (8) aggregate neighbor information for homogeneous and multi-relational graphs, respectively.  $\mathbf{W}_{\delta(u)}^k$  and  $\mathbf{W}_{\lambda(u)}^k$  encode parts of the link information as discussed in the following paragraph. For multi-relational graphs, neighboring nodes from different edge types should impose different influence for the center node during message passing. Thus, we utilize the edge embedding  $\mathbf{h}_e^k$  in (8) to further encode the type of links, where  $\mathbf{h}_e^k$  is updated by  $\mathbf{h}_e^{k+1} = \mathbf{W}_{rel}^k \mathbf{h}_e^k$ . And we incorporate the composition operator  $\phi(\cdot)$  to encode the relationship between edge embedding  $\mathbf{h}_e^k$  with node embedding  $\mathbf{h}_u^k$ . We highlight the differences between the standard MPNN space (see (1) in Sec. 2.2) with (7), (8) and (9) as follows:

- **Linear Transformation  $\mathbf{W}^k$ :** Given the hidden representation from the last layer, we first apply linear transformation towards embeddings. In (7), we assign neighborhood-type specific weight matrices  $\mathbf{W}_{\delta(u)}^k$ , where  $\delta(u) \in \{self, neigh\}$ .  $\mathbf{W}_{self}^k$ ,  $\mathbf{W}_{neigh}^k$  are introduced for the node itself and neighbors respectively. This is a weak attention mechanism towards the basic link information for homogeneous graphs, which can distinguish edges between self-type and neighbor-type. In multi-relational graphs, we use edge-aware filters  $\mathbf{W}_{\lambda(e)}^k$ , where  $\lambda(e) \in \{self\_loop, original, inverse\}$  encodes the direction information of edge  $e$ . We use  $\mathbf{W}_{sl}^k$ ,  $\mathbf{W}_O^k$ ,  $\mathbf{W}_I^k$  for self-loop, original, and inverse edge separately.

- **Composition Operator  $\phi^k$  and Edge Embedding  $\mathbf{h}_e^k$ :** Following CompGCN [Vashisht et al., 2019], we utilize the composition operator  $\phi(\mathbf{h}_u^k, \mathbf{h}_e^k)$  to capture message between the node and edge embeddings before aggregation step. While CompGCN empirically selects the most proper  $\phi(\cdot)$  through grid search, we introduce this novel design dimension into our search space, so that AutoGEL is able to search for the most suitable one together with other design dimensions in a more efficient way. Specifically, we incorporate the candidate operators  $\{sub, mult, corr\}$ , where  $sub(\cdot) = \mathbf{h}_u^k - \mathbf{h}_e^k$  [Bordes et al., 2013],  $mult(\cdot) = \mathbf{h}_u^k * \mathbf{h}_e^k$  [Yang et al., 2014],  $corr(\cdot) = \mathbf{h}_u^k \star \mathbf{h}_e^k$  [Nickel et al., 2016]. Together with  $\mathbf{W}_{\lambda(e)}^k$ , the search design on  $\phi(\mathbf{h}_u^k, \mathbf{h}_e^k)$  enables AutoGEL to capture semantic meaningful edges by  $\mathbf{h}_e^k$ , and the interaction between nodes with edges by  $\phi(\cdot)$ . That is why AutoGEL can handle the LP task on multi-relational graphs, while another edge-level model [You et al., 2020] cannot (see Tab. 1).

### 3.1.2 Inter-Layer Message Passing Design

Traditional MPNNs follows the way in (1), i.e., the input of each MPNN layer is the output of last layer. Motivated by [Xu et al., 2018a, Li et al., 2019], it is beneficial to use the combination of previous layers as input to each layer. In this paper, we also design the inter-layer search space to enables the flexible and powerful GNN architecture to be searched. Specifically, we provide two design dimensions: layer connectivity and layer aggregation.

- **Layer Connectivity:** The literature [Li et al., 2019] have shown that incorporating skip connections (i.e., residual connections and dense connections) across MPNN layers can help alleviating the over-smoothing issue [Li et al., 2018] and empirically improve the model performance. In this work, we conduct systematical investigation towards the joint impact of skip connections together with other design dimension. We select the way of layer connectivity from the set  $\{skip, lc\_sum, lc\_concat\}$ . Moreover, the layer connectivity function is given as:

$$\mathbf{h}^{k+1} \leftarrow layer\_cnt(\mathbf{h}^k, \mathbf{h}^{k+1}) = \begin{cases} \mathbf{h}^{k+1}, & skip, \\ sum(\mathbf{h}^k, \mathbf{h}^{k+1}), & lc\_sum, \\ \mathbf{W}concat(\mathbf{h}^k, \mathbf{h}^{k+1}), & lc\_concat, \end{cases} \quad (10)$$

where  $\mathbf{h}^k$  denotes embeddings output from  $k$ -th MPNN intra-layer. As shown in Fig. 1 (b), the representation  $\mathbf{h}^k$  will be fed into  $k + 1$ -th MPNN layer to learn  $\mathbf{h}^{k+1}$ . Then, AutoGEL combines  $\mathbf{h}^k$  with  $\mathbf{h}^{k+1}$  as in (10) to form a new representation, which will be fed to the next layer. Note that another AutoGNN SANE Zhao et al. [2021] does not include  $lc\_concat$ .

- **Layer Aggregation:** JKNet [Xu et al., 2018a] shows that the layer-wise aggregation allows the adaptive representation learning. The set of candidate layer-wise aggregation defined in AutoGEL is  $\{skip, la\_concat, la\_max\}$ . Specifically, the layer aggregation function is defined as:

$$\mathbf{h} = layer\_agg(\mathbf{h}^1, \dots, \mathbf{h}^L) = \begin{cases} \mathbf{h}^L, & skip, \\ [\mathbf{h}^1 || \dots || \mathbf{h}^L], & la\_concat, \\ max(\mathbf{h}^1, \dots, \mathbf{h}^L), & la\_max. \end{cases} \quad (11)$$

Note that  $layer\_agg$  aggregates the representations generated from MPNN layers, i.e., those that have not been processed by  $layer\_cnt$  (Fig. 1 (b)). And previous AutoGNNs NAS-GCN [Jiang and Balaprakash, 2020] and [You et al., 2020] do not include this operator  $layer\_agg$ .

### 3.1.3 Pooling

After the intra-layer (Sec. 3.1.1) and inter-layer (Sec. 3.1.2) message passing stages, pooling operation  $\mathbf{h}_x = R(\{\mathbf{h}_v | v \in \mathcal{X}\})$  induces high-level representations, where  $x$  and  $\mathcal{X}$  depend on the given task.

For LP task on homogeneous graphs, the pooling operation outputs the representations of links. In SEAL [Zhang and Chen, 2018], subgraph-level sortpooling method is utilized to readout information from the entire enclosing subgraph for the target link. It is proved in [Srinivasan and Ribeiro, 2019] that joint prediction task only requires joint structure representations of target node-set  $S$ . Thus, it is not necessary to introduce complex subgraph-level pooling methods. We following DE-GNN [Li et al., 2020] to learn link representations by readout only from target node-set, i.e.,  $\mathbf{h}_e = R(\{\mathbf{h}_v | v \in S\})$ . Note that the original setting difference-pooling for  $R(\cdot)$  in DE-GNN does

not achieve competitive performance in the empirical study. Instead, we provide the powerful pooling operations  $\{sum, max, concat\}$  to be selected for  $R(\cdot)$ . As for multi-relational graphs, the pooling stage is not required since the edge embedding  $\mathbf{h}_e$  is learned in the intra-layer MPNN.

For the node classification task, AutoGEL simply removes  $R(\cdot)$  from the search space as literature does. For the graph classification task, the pooling operation outputs high-level graph representation  $\mathbf{h}_G = R(\{\mathbf{h}_v | v \in G\})$ , and  $R(\cdot) \in \{global\_add\_pool, global\_mean\_pool, global\_max\_pool\}$ .

### 3.2 Search Algorithm

Given a candidate set  $\mathcal{O}$  for a specific operator (e.g.,  $\{sum, mean, max\}$  for  $AGG_k$ ), let  $\mathbf{x}$  be the hidden vector to be fed into this operator, and  $\alpha_o$  records the weight that operation  $o \in \mathcal{O}$  to be selected. Then the output from this operator is computed as  $\bar{o}(\mathbf{x}) = \sum_{o \in \mathcal{O}} \theta_o \cdot o(\mathbf{x})$ , where  $\theta_o \in \{0, 1\}$ . There are multiple operators in AutoGEL’s space (see Sec. 3.1), including intra-layer level operators (i.e.,  $\phi^k, \mathbf{W}^k, AGG_k, COM_k, ACT_k$ ), inter-layer operators (i.e.,  $layer\_cnt, layer\_agg$ ), and pooling operator  $R(\cdot)$ . Let  $\theta$  denote the operation selection for all operators. The GNN search problem can be formulated as  $\max_{\theta, \omega} f(\theta, \omega; D)$ , where  $f(\cdot)$  evaluates the performance of a GNN model  $\theta$  with weight  $\omega$  on the graph data  $D$ .

As discussed in Sec. 2.2, the search algorithm adopted in existing AutoGNNs suffers from several issues. Especially, the most similar prior work SANE [Zhao et al., 2021] adopts DARTS [Liu et al., 2018], which directly relaxes  $\theta$  to be continuous and makes the objective  $f(\theta, \omega; D)$  deterministic differentiable. However, several drawbacks brought by the mixed strategy of DARTS [Liu et al., 2018] have been observed and discussed in the community of neural architecture search. The mixed strategy usually leads to the inconsistent performance issue, i.e., the performance of the derived child network at the end of the searching stage shows significant degradation compared with the performance of the parent network before architecture derivation. That is because the relaxed  $\theta$  cannot converge to a one-hot vector [Zela et al., 2019, Chu et al., 2020], thus removing those operations at the end of search actually lead to a different architecture from the final searching result. Moreover, the mixed strategy must maintain all operators in the whole supernet, which requires more computational resources than the one-hot vector [Yao et al., 2020].

Fortunately, SNAS [Xie et al., 2018] leverages the concrete distribution [Maddison et al., 2016, Jang et al., 2016] to propose a stochastic differentiable algorithm, which enables the search objective differentiable with the reparameterization trick. Let a GNN model  $\theta$  being sampled from the distribution  $p_\alpha(\theta)$  that parameterized by the structure parameter  $\alpha$  as:

$$\theta_o = \frac{\exp((\log \alpha_o - \log(-\log(U_o)))/\tau)}{\sum_{o' \in \mathcal{O}} \exp((\log \alpha_{o'} - \log(-\log(U_{o'})))/\tau)}, \quad (12)$$

where  $\tau$  is the temperature of softmax, and  $U_o$  is sampled from the uniform distribution, i.e.,  $U_o \sim Uniform(0, 1)$ . It has been proven that  $p(\lim_{\tau \rightarrow 0} \theta_o = 1) = \alpha_o / \sum_{o' \in \mathcal{O}} \alpha_{o'}$  [Maddison et al., 2016]. This first guarantees that the probability of  $o$  being sampled (i.e.,  $\theta_o = 1$ ) is proportional to its weight  $\alpha_o$ . Besides, the one-hot property  $\lim_{\tau \rightarrow 0} \theta_o = 1$  makes the stochastic differentiable relaxation unbiased once converged [Xie et al., 2018]. Then the GNN searching problem is reformulated into  $\max_{\alpha, \omega} \mathbb{E}_{\theta \sim p_\alpha(\theta)} [f(\theta, \omega; D)]$ , where  $\mathbb{E}[\cdot]$  is the expectation. We leverage SNAS [Xie et al., 2018] to optimize the weight of GNN  $\omega$  and the weight of operator  $\alpha$ .

## 4 Experiments

### 4.1 Experimental Setting

AutoGEL<sup>2</sup> is implemented on top of code provided in DE-GNN [Li et al., 2020] and CompGCN [Vashishth et al., 2019] using Pytorch framework [Paszke et al., 2019]. All the experiments are performed using one single RTX 2080 Ti GPU. More details about data sets, hyper-parameter settings and search space designs are introduced in Appendix A.1.1, A.1.2 and A.1.3, respectively.

**Task and Data sets.** For LP task on homogeneous graphs, we follow [Zhang and Chen, 2018, Li et al., 2020] to utilize the datasets: NS [Newman, 2006], Power [Watts and Strogatz, 1998], Router

<sup>2</sup>Code is available at <https://github.com/zwangeo/AutoGEL>

Table 2: Average AUC (with standard deviation) for LP task on homogeneous graphs

Type	Model	NS	Power	Router	C.ele	USAir	Yeast	PB
Heuristic	CN	94.42±0.95	58.80±0.88	56.43±0.52	85.13±1.61	93.80±1.22	89.37±0.61	92.04±0.35
	RA	94.45±0.93	58.79±0.88	56.43±0.51	87.49±1.41	95.77±0.92	89.45±0.62	92.46±0.37
	Katz	94.85±1.10	65.39±1.59	38.62±1.35	86.34±1.89	92.88±1.42	92.24±0.61	92.92±0.35
Latent	SPC	89.94±2.39	91.78±0.61	68.79±2.42	51.90±2.57	74.22±3.11	93.25±0.40	83.96±0.86
	LINE	80.63±1.90	55.63±1.47	67.15±2.10	69.21±3.14	81.47±10.71	87.45±3.33	76.95±2.76
	N2V	91.52±1.28	76.22±0.92	65.46±0.86	84.11±1.27	91.44±1.78	93.67±0.46	85.79±0.78
GLP	VGAE	94.04±1.64	71.20±1.65	61.51±1.22	81.80±2.18	89.28±1.99	93.88±0.21	90.70±0.53
	PGNN	94.88±0.77	-	-	78.20±0.33	-	-	89.72±0.32
	SEAL	98.85±0.47	87.61±1.57	96.38±1.45	90.30±1.35	96.62±0.72	97.91±0.52	94.72±0.46
	DE-GNN	99.09±0.79	96.68±0.29	98.69±0.17	89.37±0.17	98.04±0.66	98.59±0.26	94.95±0.37
AutoGNN	AutoGEL	<b>99.89±0.06</b>	<b>98.00±0.21</b>	<b>99.08±0.28</b>	<b>92.90±1.02</b>	<b>98.49±0.45</b>	<b>99.24±0.10</b>	<b>97.27±0.15</b>

[Spring et al., 2002], C.ele [Watts and Strogatz, 1998], USAir [Batagelj and Mrvar, 2009], Yeast [Von Mering et al., 2002] and PB [Ackland et al., 2005]. As for the LP task on multi-relational graphs, we mainly adopt benchmark knowledge graphs (KGs), FB15k-237 [Toutanova and Chen, 2015] and WN18RR [Dettmers et al., 2018].

For the node classification task, we compare models on three popular citation networks [Sen et al., 2008], i.e., Cora, CiteSeer, and PubMed. For the graph classification task, we adopt four standard benchmarks [Yanardag and Vishwanathan, 2015]: 1) social network datasets: IMDB-BINARY and IMDB-MULTI, 2) bioinformatics datasets: MUTAG and PROTEINS.

**Evaluation Metrics.** For node classification and graph classification, we adopt average accuracy as measurement. We report AUC with standard deviation for LP task on homogeneous graphs. For LP on KGs, we adopt standard evaluation matrices:

- Mean Reciprocal Ranking (MRR):  $(\sum_{i=1}^{|S|} 1/rank_i)/|S|$ , where  $S$  and  $rank_i$  denote test triples and ranking results, respectively
- Hits@N:  $(\sum_{i=1}^{|S|} \mathbb{1}(rank_i \leq N))/|S|$ , where  $\mathbb{1}$  denotes indicator function, and  $N \in \{1, 3, 10\}$ .

**Baselines.** For LP on homogeneous graphs, we use the following approaches as baselines: 1) heuristic methods: CN [Bütün et al., 2018], RA [Zhou et al., 2009], and Katz [Katz, 1953], 2) latent feature based methods: Spectral clustering (SPC) [Tang and Liu, 2011], LINE [Tang et al., 2015] and node2vec (N2V) [Grover and Leskovec, 2016], 3) GLP methods: VGAE [Kipf and Welling, 2016b], PGNN [You et al., 2019], SEAL [Zhang and Chen, 2018], and DE-GNN [Li et al., 2020].

For LP on KGs, we compare AutoGEL with several KG embedding approaches: 1) the geometric models: TransE [Bordes et al., 2013] and RotatE [Sun et al., 2019], 2) bilinear models: DistMult [Yang et al., 2014] and ComplEx [Trouillon et al., 2016], 3) GLP models: R-GCN [Kipf and Welling, 2016b], SACN [Shang et al., 2019], VR-GCN [Ye et al., 2019] and CompGCN [Vashishth et al., 2019], 4) other NN-based models: ConvKB [Nguyen et al., 2017], ConvE [Dettmers et al., 2018], ConvR [Jiang et al., 2019] and HyperER [Balažević et al., 2019].

For the node classification task, we compare AutoGEL with the following baselines: 1) manually designed GNNs: GCN [Kipf and Welling, 2016a], GraphSAGE [Hamilton et al., 2017], GAT [Veličković et al., 2017] and GIN [Xu et al., 2018b], 2) AutoGNNs: GraphNAS [Gao et al., 2020], SANE [Zhao et al., 2021] and [You et al., 2020]. AGNN Zhou et al. [2019] is not included due to no available code.

For the graph classification task, we compare AutoGEL with the following baselines: 1) manually designed GNNs: PATCHY-SAN [Niepert et al., 2016], DGCNN [Zhang et al., 2018], GCN [Kipf and Welling, 2016a], GraphSAGE [Hamilton et al., 2017] and GIN [Xu et al., 2018b], 2) AutoGNNs: [You et al., 2020]. Note that NAS-GCN is specifically designed for molecular property prediction, which is not included in the comparison.

## 4.2 Comparison with GLP models

The model comparison for LP task on homogeneous graphs and knowledge graphs have been summarized in Tab. 2 and 3, respectively. As shown in Tab. 2, heuristic methods perform well on several datasets, but they fail to handle data sets Power and Router. Latent feature-based methods improve the performance on these two data sets but cannot achieve competitive results on other



Table 3: MRR and Hits@N for LP task on knowledge graphs

Type	Model	FB15k-237				WN18RR			
		MRR	Hits@10	Hits@3	Hits@1	MRR	Hits@10	Hits@3	Hits@1
Geometric	TransE	.294	.465	-	-	.226	.501	-	-
	RotatE	.338	.533	.375	.241	<u>.476</u>	<b>.571</b>	<u>.492</u>	.428
Bilinear	DisMult	.241	.419	.263	.155	.430	.490	.440	.390
	CompLex	.247	.428	.275	.158	.440	.510	.460	.410
NN-based	ConvKB	.243	.421	.371	.155	.249	.524	.417	.057
	ConvE	.325	.501	.356	.237	.430	.520	.440	.400
	ConvR	.350	.528	.385	.261	.475	.537	.489	<u>.443</u>
	HyperER	.341	.520	.376	.252	.465	.522	.477	.436
GLP	R-GCN	.248	.417	-	.151	-	-	-	-
	SACN	.350	<b>.540</b>	<u>.390</u>	.260	.470	.540	.480	.430
	VR-GCN	.248	.432	.272	.159	-	-	-	-
	CompGCN	<u>.355</u>	.535	<u>.390</u>	<u>.264</u>	<b>.479</b>	.546	<b>.494</b>	<u>.443</u>
AutoGNN	AutoGEL	<b>.357</b>	<u>.538</u>	<b>.391</b>	<b>.266</b>	<b>.479</b>	<u>.549</u>	<u>.492</u>	<b>.444</b>

Table 4: Average accuracy (%) for node classification and graph classification

Type	Model	Node Classification			Graph Classification			
		Cora	CiteSeer	Pubmed	IMDB-B	IMDB-M	MUTAG	PROTEINS
Manual GNNs	PATCHYSAN	-	-	-	71.00	45.20	<u>92.60</u>	75.90
	DGCNN	-	-	-	70.00	47.80	85.80	75.50
	GCN	88.11	76.66	88.58	74.00	51.90	85.60	76.00
	GraphSAGE	87.41	75.99	88.34	72.30	50.90	85.10	75.90
	GAT	87.19	75.18	85.73	-	-	-	-
	GIN	86.00	73.40	87.99	<u>75.10</u>	<u>52.30</u>	89.40	<u>76.20</u>
AutoGNN	GraphNAS	88.40	77.62	88.96	-	-	-	-
	SANE	<u>89.26</u>	<b>78.59</b>	<b>90.47</b>	-	-	-	-
	You et al. [2020]	88.50	74.90	-	-	47.80	-	73.90
	AutoGEL	<b>89.89</b>	<u>77.66</u>	<u>89.68</u>	<b>81.20</b>	<b>56.80</b>	<b>94.74</b>	<b>82.68</b>

data sets. GLP models outperform heuristic methods and latent feature-based methods, showing their superiority towards LP task. Specifically, DE-GNN is our strongest baseline, where vanilla GCN is adopted to learn node representations for all datasets, then link representation is induced by pooling node embeddings in (4). However, DE-GNN fails to handle the data-diversity issue and cannot consistently achieve leading performance on all data sets. In this paper, AutoGEL first adopts the pooling way in DE-GNN, then enables a more flexible way to select the most suitable pooling function  $R(\cdot)$  (see Sec. 3.1.3) instead of the fixed pooling function in DE-GNN. Searching the pooling function and other operators make AutoGEL handle the data-diversity issue, and consistently achieve the state-of-the-art performance for LP task on homogeneous graphs. Furthermore, we demonstrate the model performance of LP task on knowledge graphs in Tab. 3. Note that the improvements on KGs is not as obvious as that on homogeneous graphs. In practice, GLP models run longer than Geometric and Bilinear models, which leads to the difficulty of tuning hyper-parameters (see more discussions in Appendix A.4).

Moreover, we present several cases of searched architectures in Appendix A.2. And we show several ablation studies to provide some insights into the AutoGEL space design in Appendix A.3, including the impacts of the inter-level design, pooling operator, weight transformation matrices, and edge embedding.

### 4.3 Comparison with AutoGNN models

To compare with other AutoGNNs, we also demonstrate the performance of AutoGEL on node-level and graph-level tasks. The empirical comparison on the node classification and graph classification task is shown in Tab. 4. AutoGEL shows the great generalization ability towards different graph tasks. AutoGEL outperforms all the manually designed GNN baselines and also achieves competitive results with existing AutoGNNs designed specifically for these tasks. The data sets for node classification

Table 5: The search time (clock time in seconds) of AutoGNNs on the node classification task.

Model	Cora	Citeseer	PubMed
GraphNAS [Gao et al., 2020]	3240	3665	5917
SANE [Zhao et al., 2021]	14	35	54
AutoGEL	12	16	19

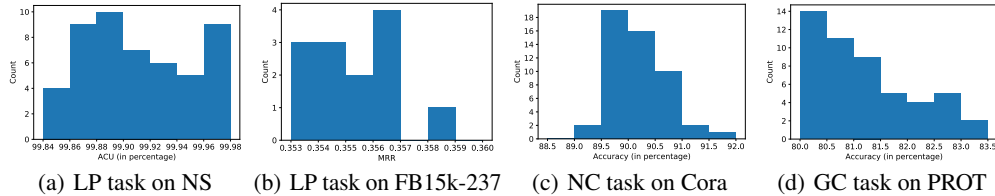


Figure 2: Performance frequency statistics over multiple runs for each task

task usually contains rich node features. AutoGEL simplifies the attention mechanism in existing GNNs for node classification from  $a_{uv}$  (see Sec. 2.2) to  $\mathbf{W}_{\delta(u)}^k$  in (7), which leads to slightly inadequate performance. We notice that AutoGEL brings more significant performance gains on the graph classification task. The data sets for graph classification have not sufficient node features as those data sets for node classification, which requires effective learning from graph structures. AutoGEL is more suitable for this task by learning from edges.

We also compare the search efficiency between AutoGNNs in Tab. 5. Statistics for other AutoGNNs are taken from the start-of-the-art SANE [Zhao et al., 2021], which sets search epochs to 200 for all the AutoGNN baselines. To reduce search cost in GraphNAS, SANE and AutoGEL leverages the idea of parameter sharing Pham et al. [2018] to avoid repeatedly training weights of different sampled GNN architectures. Moreover, AutoGEL adopts a more advanced search algorithm compared with SANE (see Sec. 3.2), thereby further reduces the search cost. We show experimental results of a variant of AutoGEL in search algorithm in Appendix A.3. And more details about search efficiency are reported in Appendix A.4.

#### 4.4 The Empirical Study on Robustness

All effectiveness results in the main context (Tab. 2, Tab. 3, and Tab. 4) are reported under the average of 4 runs. Note that Tab. 3 and Tab. 4 do not contain variance due to space limits. To illustrate the robustness of AutoGEL, here we report results after multiple runs of AutoGEL on several tasks in Fig. 2. We set the number of different runs as 10 for FB15k-237 dataset and 50 for the rest, due to the relative longer running time required for FB15k-237. We can see that even in the some worst cases, AutoGEL still rival or surpass its strongest baselines over all the tasks, its indicating the effectiveness.

## 5 Conclusion

In this paper, we present a novel AutoGNN with explicit link information, named AutoGEL. Specifically, AutoGEL incorporates the edge embedding in the MPNN space, and proposes several novel design dimensions at intra-layer and inter-layer designs. Moreover, AutoGEL upgrades the search algorithm of AutoGNNs by leveraging a promising NAS algorithm SNAS. Experimental results well demonstrate that AutoGEL not only achieves the leading performance on the LP task, but also shows competitive results on the node and graph classification tasks.

For future works, one direction worth trying is to adapt AutoGNNs to the LP task on hyper-relational KGs, which contain a lot of hyper-relational facts  $r(u_1, \dots, u_n), n \geq 2$ . First, the pioneer data-aware methods for LP tasks on KGs are mainly based on the bilinear models, such as AutoSF [Zhang et al., 2020c] and ERAS [Shimin et al., 2021]. Introducing the MPNN space can promote a more comprehensive search space because the composition operator is not limited to the bilinear models. Second, using the multi-relational hypergraph could be a more natural way to model hyper-relational facts [Yadati, 2020, Di et al., 2021]. Another interesting direction is to search GNN architectures on

dynamic graph data sets. Note that search efficiency would be the most challenging issue. One of the key points is to make full use of previous well-trained GNN controllers.

## 6 Acknowledgements

Lei Chen’s work is partially supported by National Key Research and Development Program of China Grant No. 2018AAA0101100, the Hong Kong RGC GRF Project 16202218, CRF Project C6030-18G, C1031-18G, C5026-18G, RIF Project R6020-19, AOE Project AoE/E-603/18, Theme-based project TRS T41-603/20R, China NSFC No. 61729201, Guangdong Basic and Applied Basic Research Foundation 2019B151530001, Hong Kong ITC ITF grants ITS/044/18FX and ITS/470/18FX, Microsoft Research Asia Collaborative Research Grant, HKUST-NAVER/LINE AI Lab, Didi-HKUST joint research lab, HKUST-Webank joint research lab grants.

## References

- Zhan Bu, Jie Cao, Hui-Jia Li, Guangliang Gao, and Haicheng Tao. Gleam: A graph clustering framework based on potential game optimization for large-scale social networks. *Knowledge and Information Systems*, 55(3):741–770, 2018.
- Alvaro Sanchez-Gonzalez, Nicolas Heess, Jost Tobias Springenberg, Josh Merel, Martin Riedmiller, Raia Hadsell, and Peter Battaglia. Graph networks as learnable physics engines for inference and control. In *ICML*, pages 4470–4479. PMLR, 2018.
- Xiang Yue, Zhen Wang, Jingong Huang, Srinivasan Parthasarathy, Soheil Moosavinasab, Yungui Huang, Simon M Lin, Wen Zhang, Ping Zhang, and Huan Sun. Graph embedding on biomedical networks: methods, applications and evaluations. *Bioinformatics*, 36(4):1241–1251, 2020.
- Thomas N Kipf and Max Welling. Semi-supervised classification with graph convolutional networks. *arXiv preprint arXiv:1609.02907*, 2016a.
- William L Hamilton, Rex Ying, and Jure Leskovec. Inductive representation learning on large graphs. *arXiv preprint arXiv:1706.02216*, 2017.
- Shikhar Vashishth, Soumya Sanyal, Vikram Nitin, and Partha Talukdar. Composition-based multi-relational graph convolutional networks. *arXiv preprint arXiv:1911.03082*, 2019.
- Pan Li, Yanbang Wang, Hongwei Wang, and Jure Leskovec. Distance encoding: Design provably more powerful neural networks for graph representation learning. *NeurIPS*, 33, 2020.
- Mathias Niepert, Mohamed Ahmed, and Konstantin Kutikov. Learning convolutional neural networks for graphs. In *ICML*, pages 2014–2023. PMLR, 2016.
- Muhan Zhang, Zhicheng Cui, Marion Neumann, and Yixin Chen. An end-to-end deep learning architecture for graph classification. In *AAAI*, volume 32, 2018.
- Jiaxuan You, Zhitao Ying, and Jure Leskovec. Design space for graph neural networks. *NeurIPS*, 33, 2020.
- Justin Gilmer, Samuel S Schoenholz, Patrick F Riley, Oriol Vinyals, and George E Dahl. Neural message passing for quantum chemistry. In *ICML*, pages 1263–1272. PMLR, 2017.
- Thomas Elsken, Jan Hendrik Metzen, Frank Hutter, et al. Neural architecture search: A survey. *J. Mach. Learn. Res.*, 20(55):1–21, 2019.
- Kaixiong Zhou, Qingquan Song, Xiao Huang, and Xia Hu. Auto-gnn: Neural architecture search of graph neural networks. *arXiv preprint arXiv:1909.03184*, 2019.
- Yang Gao, Hong Yang, Peng Zhang, Chuan Zhou, and Yue Hu. Graph neural architecture search. In *IJCAI*, volume 20, pages 1403–1409, 2020.
- Shengli Jiang and Prasanna Balaprakash. Graph neural network architecture search for molecular property prediction. *arXiv preprint arXiv:2008.12187*, 2020.

- Huan Zhao, Quanming Yao, and Weiwei Tu. Search to aggregate neighborhood for graph neural network. ICDE, 2021.
- Yuhui Ding, Quanming Yao, Huan Zhao, and Tong Zhang. Diffmg: Differentiable meta graph search for heterogeneous graph neural networks. In SIGKDD, pages 279–288, 2021.
- Lanning Wei, Huan Zhao, Quanming Yao, and Zhiqiang He. Pooling architecture search for graph classification. CIKM, 2021.
- Ronald J Williams. Simple statistical gradient-following algorithms for connectionist reinforcement learning. Machine learning, 8(3-4):229–256, 1992.
- Hanxiao Liu, Karen Simonyan, and Yiming Yang. Darts: Differentiable architecture search. arXiv preprint arXiv:1806.09055, 2018.
- Sirui Xie, Hehui Zheng, Chunxiao Liu, and Liang Lin. Snas: stochastic neural architecture search. arXiv preprint arXiv:1812.09926, 2018.
- Michael Schlichtkrull, Thomas N Kipf, Peter Bloem, Rianne Van Den Berg, Ivan Titov, and Max Welling. Modeling relational data with graph convolutional networks. In European semantic web conference, pages 593–607. Springer, 2018.
- Yongqi Zhang, Quanming Yao, Yingxia Shao, and Lei Chen. Nscaching: simple and efficient negative sampling for knowledge graph embedding. In ICDE, pages 614–625. IEEE, 2019.
- Yongqi Zhang, Quanming Yao, and Lei Chen. Interstellar: Searching recurrent architecture for knowledge graph embedding. NeurIPS, 33:10030–10040, 2020a.
- Zhilin Yang, William Cohen, and Ruslan Salakhudinov. Revisiting semi-supervised learning with graph embeddings. In ICML, pages 40–48. PMLR, 2016.
- Kristina Toutanova and Danqi Chen. Observed versus latent features for knowledge base and text inference. In Proceedings of the 3rd workshop on continuous vector space models and their compositionality, pages 57–66, 2015.
- Muhan Zhang, Pan Li, Yinglong Xia, Kai Wang, and Long Jin. Revisiting graph neural networks for link prediction. arXiv preprint arXiv:2010.16103, 2020b.
- Muhan Zhang and Yixin Chen. Link prediction based on graph neural networks. arXiv preprint arXiv:1802.09691, 2018.
- Bryan Perozzi, Rami Al-Rfou, and Steven Skiena. Deepwalk: Online learning of social representations. In SIGKDD, pages 701–710, 2014.
- Aditya Grover and Jure Leskovec. node2vec: Scalable feature learning for networks. In SIGKDD, pages 855–864, 2016.
- Thomas N Kipf and Max Welling. Variational graph auto-encoders. arXiv preprint arXiv:1611.07308, 2016b.
- Diego Marcheggiani and Ivan Titov. Encoding sentences with graph convolutional networks for semantic role labeling. arXiv preprint arXiv:1703.04826, 2017.
- Chao Shang, Yun Tang, Jing Huang, Jinbo Bi, Xiaodong He, and Bowen Zhou. End-to-end structure-aware convolutional networks for knowledge base completion. In AAAI, volume 33, pages 3060–3067, 2019.
- Antoine Bordes, Nicolas Usunier, Alberto Garcia-Duran, Jason Weston, and Oksana Yakhnenko. Translating embeddings for modeling multi-relational data. In NIPS, pages 1–9, 2013.
- Bishan Yang, Wen-tau Yih, Xiaodong He, Jianfeng Gao, and Li Deng. Embedding entities and relations for learning and inference in knowledge bases. arXiv preprint arXiv:1412.6575, 2014.
- Maximilian Nickel, Lorenzo Rosasco, and Tomaso Poggio. Holographic embeddings of knowledge graphs. In AAAI, volume 30, 2016.

- Keyulu Xu, Chengtao Li, Yonglong Tian, Tomohiro Sonobe, Ken-ichi Kawarabayashi, and Stefanie Jegelka. Representation learning on graphs with jumping knowledge networks. In *ICML*, pages 5453–5462. PMLR, 2018a.
- Guohao Li, Matthias Muller, Ali Thabet, and Bernard Ghanem. Deepgens: Can gcns go as deep as cnns? In *Proceedings of the IEEE/CVF International Conference on Computer Vision*, pages 9267–9276, 2019.
- Qimai Li, Zhichao Han, and Xiao-Ming Wu. Deeper insights into graph convolutional networks for semi-supervised learning. In *AAAI*, volume 32, 2018.
- Balasubramaniam Srinivasan and Bruno Ribeiro. On the equivalence between positional node embeddings and structural graph representations. *arXiv preprint arXiv:1910.00452*, 2019.
- Arber Zela, Thomas Elsken, Tonmoy Saikia, Yassine Marrakchi, Thomas Brox, and Frank Hutter. Understanding and robustifying differentiable architecture search. *arXiv preprint arXiv:1909.09656*, 2019.
- Xiangxiang Chu, Tianbao Zhou, Bo Zhang, and Jixiang Li. Fair darts: Eliminating unfair advantages in differentiable architecture search. In *ECCV*, pages 465–480. Springer, 2020.
- Quanming Yao, Ju Xu, Wei-Wei Tu, and Zhanxing Zhu. Efficient neural architecture search via proximal iterations. In *AAAI*, volume 34, pages 6664–6671, 2020.
- Chris J Maddison, Andriy Mnih, and Yee Whye Teh. The concrete distribution: A continuous relaxation of discrete random variables. *arXiv preprint arXiv:1611.00712*, 2016.
- Eric Jang, Shixiang Gu, and Ben Poole. Categorical reparameterization with gumbel-softmax. *arXiv preprint arXiv:1611.01144*, 2016.
- Adam Paszke, Sam Gross, Francisco Massa, Adam Lerer, James Bradbury, Gregory Chanan, Trevor Killeen, Zeming Lin, Natalia Gimelshein, Luca Antiga, et al. Pytorch: An imperative style, high-performance deep learning library. *arXiv preprint arXiv:1912.01703*, 2019.
- Mark EJ Newman. Finding community structure in networks using the eigenvectors of matrices. *Physical review E*, 74(3):036104, 2006.
- Duncan J Watts and Steven H Strogatz. Collective dynamics of ‘small-world’ networks. *nature*, 393(6684):440–442, 1998.
- Neil Spring, Ratul Mahajan, and David Wetherall. Measuring isp topologies with rocketfuel. *SIGCOMM*, 32(4):133–145, 2002.
- Vladimir Batagelj and Andrej Mrvar. Pajek datasets (2006), 2009.
- Christian Von Mering, Roland Krause, Berend Snel, Michael Cornell, Stephen G Oliver, Stanley Fields, and Peer Bork. Comparative assessment of large-scale data sets of protein–protein interactions. *Nature*, 417(6887):399–403, 2002.
- Robert Ackland et al. Mapping the us political blogosphere: Are conservative bloggers more prominent? In *BlogTalk Downunder 2005 Conference, Sydney*. BlogTalk Downunder 2005 Conference, Sydney, 2005.
- Tim Dettmers, Pasquale Minervini, Pontus Stenetorp, and Sebastian Riedel. Convolutional 2d knowledge graph embeddings. In *AAAI*, volume 32, 2018.
- Prithviraj Sen, Galileo Namata, Mustafa Bilgic, Lise Getoor, Brian Galligher, and Tina Eliassi-Rad. Collective classification in network data. *AI magazine*, 29(3):93–93, 2008.
- Pinar Yanardag and SVN Vishwanathan. Deep graph kernels. In *SIGKDD*, pages 1365–1374, 2015.
- Ertan Büttün, Mehmet Kaya, and Reda Alhaji. Extension of neighbor-based link prediction methods for directed, weighted and temporal social networks. *Information Sciences*, 463:152–165, 2018.

- Tao Zhou, Linyuan Lü, and Yi-Cheng Zhang. Predicting missing links via local information. The European Physical Journal B, 71(4):623–630, 2009.
- Leo Katz. A new status index derived from sociometric analysis. Psychometrika, 18(1):39–43, 1953.
- Lei Tang and Huan Liu. Leveraging social media networks for classification. Data Mining and Knowledge Discovery, 23(3):447–478, 2011.
- Jian Tang, Meng Qu, Mingzhe Wang, Ming Zhang, Jun Yan, and Qiaozhu Mei. Line: Large-scale information network embedding. In WWW, pages 1067–1077, 2015.
- Jiaxuan You, Rex Ying, and Jure Leskovec. Position-aware graph neural networks. In ICML, pages 7134–7143. PMLR, 2019.
- Zhiqing Sun, Zhi-Hong Deng, Jian-Yun Nie, and Jian Tang. Rotate: Knowledge graph embedding by relational rotation in complex space. arXiv preprint arXiv:1902.10197, 2019.
- Théo Trouillon, Johannes Welbl, Sebastian Riedel, Éric Gaussier, and Guillaume Bouchard. Complex embeddings for simple link prediction. In ICML, pages 2071–2080. PMLR, 2016.
- Rui Ye, Xin Li, Yujie Fang, Hongyu Zang, and Mingzhong Wang. A vectorized relational graph convolutional network for multi-relational network alignment. In IJCAI, pages 4135–4141, 2019.
- Dai Quoc Nguyen, Tu Dinh Nguyen, Dat Quoc Nguyen, and Dinh Phung. A novel embedding model for knowledge base completion based on convolutional neural network. arXiv preprint arXiv:1712.02121, 2017.
- Xiaotian Jiang, Quan Wang, and Bin Wang. Adaptive convolution for multi-relational learning. In Proceedings of the 2019 Conference of the North American Chapter of the Association for Computational Linguistics: Human Language Technologies, Volume 1 (Long and Short Papers), pages 978–987, 2019.
- Ivana Balažević, Carl Allen, and Timothy M Hospedales. Hypernetwork knowledge graph embeddings. In International Conference on Artificial Neural Networks, pages 553–565. Springer, 2019.
- Petar Veličković, Guillem Cucurull, Arantxa Casanova, Adriana Romero, Pietro Lio, and Yoshua Bengio. Graph attention networks. arXiv preprint arXiv:1710.10903, 2017.
- Keyulu Xu, Weihua Hu, Jure Leskovec, and Stefanie Jegelka. How powerful are graph neural networks? arXiv preprint arXiv:1810.00826, 2018b.
- Hieu Pham, Melody Guan, Barret Zoph, Quoc Le, and Jeff Dean. Efficient neural architecture search via parameters sharing. In ICML, pages 4095–4104. PMLR, 2018.
- Yongqi Zhang, Quanming Yao, Wenyuan Dai, and Lei Chen. Autosf: Searching scoring functions for knowledge graph embedding. In ICDE, pages 433–444. IEEE, 2020c.
- DI Shimin, YAO Quanming, Yongqi ZHANG, and CHEN Lei. Efficient relation-aware scoring function search for knowledge graph embedding. In ICDE, pages 1104–1115. IEEE, 2021.
- Naganand Yadati. Neural message passing for multi-relational ordered and recursive hypergraphs. NeurIPS, 33, 2020.
- Shimin Di, Quanming Yao, and Lei Chen. Searching to sparsify tensor decomposition for n-ary relational data. In Webconf, pages 4043–4054, 2021.
- James Bergstra, Daniel Yamins, and David Cox. Making a science of model search: Hyperparameter optimization in hundreds of dimensions for vision architectures. In ICML, pages 115–123. PMLR, 2013.
- Marc Barthélémy and Luis A Nunes Amaral. Small-world networks: Evidence for a crossover picture. In The Structure and Dynamics of Networks, pages 304–307. Princeton University Press, 2011.

Matthew K Matlock, Arghya Datta, Na Le Dang, Kevin Jiang, and S Joshua Swamidass. Deep learning long-range information in undirected graphs with wave networks. In *IJCNN*, pages 1–8. IEEE, 2019.

Nima Dehmamy, Albert-László Barabási, and Rose Yu. Understanding the representation power of graph neural networks in learning graph topology. *arXiv preprint arXiv:1907.05008*, 2019.

## Checklist

1. For all authors...
  - (a) Do the main claims made in the abstract and introduction accurately reflect the paper’s contributions and scope? [\[Yes\]](#)
  - (b) Did you describe the limitations of your work? [\[Yes\]](#) Please see Section 4.2.
  - (c) Did you discuss any potential negative societal impacts of your work? [\[No\]](#) We do not think this work would have any negative societal impacts.
  - (d) Have you read the ethics review guidelines and ensured that your paper conforms to them? [\[Yes\]](#)
2. If you are including theoretical results...
  - (a) Did you state the full set of assumptions of all theoretical results? [\[N/A\]](#) We do not include theoretical analysis. We mainly focus on empirical study in this work.
  - (b) Did you include complete proofs of all theoretical results? [\[N/A\]](#)
3. If you ran experiments...
  - (a) Did you include the code, data, and instructions needed to reproduce the main experimental results (either in the supplemental material or as a URL)? [\[Yes\]](#)
  - (b) Did you specify all the training details (e.g., data splits, hyperparameters, how they were chosen)? [\[Yes\]](#) Please see Appendix A.1.1 for data splits and Appendix A.1.2 for hyperparameters.
  - (c) Did you report error bars (e.g., with respect to the random seed after running experiments multiple times)? [\[Yes\]](#) Please see Section 4.2 for standard deviation values.
  - (d) Did you include the total amount of compute and the type of resources used (e.g., type of GPUs, internal cluster, or cloud provider)? [\[Yes\]](#) Please see Section 4.1 for the GPU type. See Section 4.3 and Appendix ?? for the computation cost.
4. If you are using existing assets (e.g., code, data, models) or curating/releasing new assets...
  - (a) If your work uses existing assets, did you cite the creators? [\[Yes\]](#)
  - (b) Did you mention the license of the assets? [\[Yes\]](#) All the assets used in this work is public.
  - (c) Did you include any new assets either in the supplemental material or as a URL? [\[N/A\]](#)
  - (d) Did you discuss whether and how consent was obtained from people whose data you’re using/curating? [\[Yes\]](#) All the datasets used in this work are public.
  - (e) Did you discuss whether the data you are using/curating contains personally identifiable information or offensive content? [\[N/A\]](#) We do not involve such datasets in this work.
5. If you used crowdsourcing or conducted research with human subjects...
  - (a) Did you include the full text of instructions given to participants and screenshots, if applicable? [\[N/A\]](#) We do not conduct such research in this work.
  - (b) Did you describe any potential participant risks, with links to Institutional Review Board (IRB) approvals, if applicable? [\[N/A\]](#)
  - (c) Did you include the estimated hourly wage paid to participants and the total amount spent on participant compensation? [\[N/A\]](#)

Table 6: Dataset statistics for link prediction task

	Homogeneous Graphs							KGs	
	NS	Power	Router	C.ele	USAir	Yeast	PB	FB15k237	WN18RR
# Nodes	1589	4941	5022	297	332	2375	1222	14541	40943
# Edges	2742	6594	6258	2148	2126	11693	16714	310116	93003
# Edge types	1	1	1	1	1	1	1	237	11
# Relations	-	-	-	-	-	-	-	237	11
Avg. # Degrees	3.45	2.67	2.49	14.46	12.81	9.85	27.36	21.33	2.27
# Training	4387	10550	10012	3436	3401	18708	26742	272,115	86,835
# Validation	548	1319	1251	429	425	2338	3342	17,535	3,034
# Testing	548	1319	1251	429	425	2338	3342	20,466	3,134

Table 7: Dataset statistics for node classification and graph classification task

	Node Classification			Graph Classification			
	Cora	CiteSeer	PubMed	IMDB-B	IMDB-M	MUTAG	PROTEINS
# Graphs	1	1	1	1000	1500	188	1113
# Nodes	2708	3327	19717	19.8 (Avg.)	13.0 (Avg.)	17.9 (Avg.)	39.1 (Avg.)
# Edges	2742	6594	6258	96.53 (Avg.)	65.94 (Avg.)	19.79 (Avg.)	72.82 (Avg.)
# Edge types	1	1	1	1	1	4	1
# Node Attr.	1433	3703	500	-	-	3	7
# Classes	7	6	3	2	3	2	2

## A Experiments

### A.1 More Experimental Settings

#### A.1.1 Dataset Details

We summarize the dataset statistics in Tab. 6 and Tab. 7. In terms of dataset splits, for LP task on homogeneous graphs, we follow [Li et al., 2020] to split 80%, 10%, 10% of existing links for training, validation and testing respectively. The same number of negative links are also included through random sampling. During training phase, positive test links are removed to avoid label leakage. For KGs, we follow their standard split as shown in Tab. 6. Moreover, we use 60%, 20%, 20% dataset split for node classification as in [Zhao et al., 2021], and 80%, 10%, 10% for graph classification task to keep the same percentage of test split as in [Xu et al., 2018b] for fair comparison.

#### A.1.2 Hyperparameter Settings

We provide detailed hyperparameter settings in Tab. 8 for our implementation. Hyperparameters are tuned through hyperopt<sup>3</sup> Bergstra et al. [2013].

Table 8: List of value / range of hyperparameters in AutoGEL’s implementation

Hyperparameters	Link Prediction		Node Classification	Graph Classification
	Homo. Graphs	KGs		
Optimizer	Adam	Adam	Adam	Adam
Learning rate	1e-4	{1e-3, 1e-4}	{1e-3, 5e-3, 1e-4}	{1e-2, 1e-3, 1e-4}
MPNN layers	2	{1, 2}	2	4
Batch size	{64, 128}	{128, 256}	{64, 256}	{32, 128}
Hidden dimension	100	200	{64, 256}	{16, 32, 64}
Dropout	{0, 0.2}	{0, 0.1, 0.2, 0.3}	{0, 0.5}	{0, 0.5}
Search epoch	300	{200, 300}	{30, 200}	{30, 200}

<sup>3</sup><https://github.com/hyperopt/hyperopt>



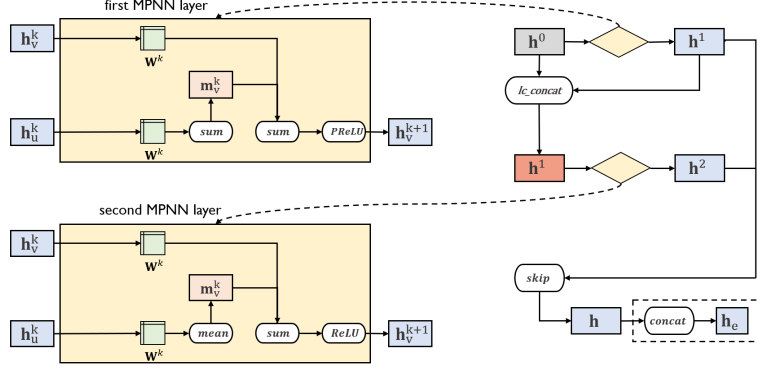


Figure 3: An example: GNN architecture searched by AutoGEL for LP task on PB dataset.

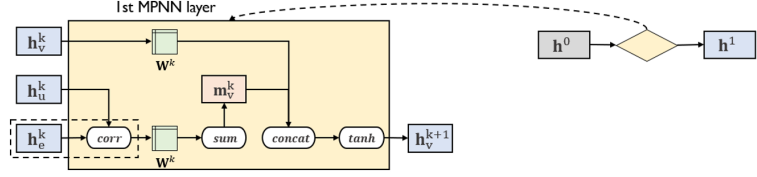


Figure 4: An example: GNN architecture searched by AutoGEL for LP task on FB15k-237 dataset.

### A.1.3 Search Space

Apart from our main designs presented in Section 3.1, AutoGEL also includes several other intra-level design dimensions in the search space:

- **Aggregation**  $AGG_k$ : We follow the common design in AutoGNN works (please refer to Section 2.2 for more details) to include  $\{sum, mean, max\}$  for neighborhood aggregation.
- **Combination**  $COM_k$ : We select combination function from  $\{sum, concat\}$ . We omit  $mlp$  combination since we empirically find simpler combination operator  $sum$  and  $concat$  adopted in our search space already achieves good performance.
- **Activation**  $ACT_k$ : Empirical observations from [You et al., 2020] shows the superiority of PReLU as the activation function for GNNs. In this work, we restrict our candidate activation functions in  $\{ReLU, PReLU\}$ . For the LP task on KGs, we follow the alternative setting to use  $tanh$  since we empirically found  $ReLU$  and  $PReLU$  not suitable.
- **Node Labeling**: The node labeling method (e.g., double-radius node labeling (DRNL) [Zhang and Chen, 2018] and distance encoding (DE) [Li et al., 2020]) is an important component towards the success of structural prediction tasks (e.g., link prediction). AutoGEL presets the DE as the node labeling approach for the LP task due to its generality and empirically good performance. DRNL can be regarded as a special case for DE, where the differences between them are marginal. Both DE and DRNL work well in practice [Li et al., 2020]. Moreover, we tried to incorporate this design dimension into the search space and enable it to be jointly searched with other architecture components. Unfortunately, sacrificing some search efficiency may not be able to improve the effectiveness because DE is already a powerful technique. Out of this concern, AutoGEL presets DE as the node labeling method to better balance between effectiveness and efficiency.

## A.2 Case Study

Here we show some searched architectures for several tasks: link prediction (LP), node classification (NC), and graph classification (GC).

For the LP task (see Fig. 3 and Fig. 4), we find that the depth of MPNN layers  $L$  leading to highest performance is different from graph scenarios. Generally,  $L = 2$  for homogeneous graphs while  $L = 1$  for knowledge graph. One possible reason is that KGs are usually more densely connected (see Tab. 6 for more dataset details), and deeper MPNN layers would cause the over-smoothing issue,

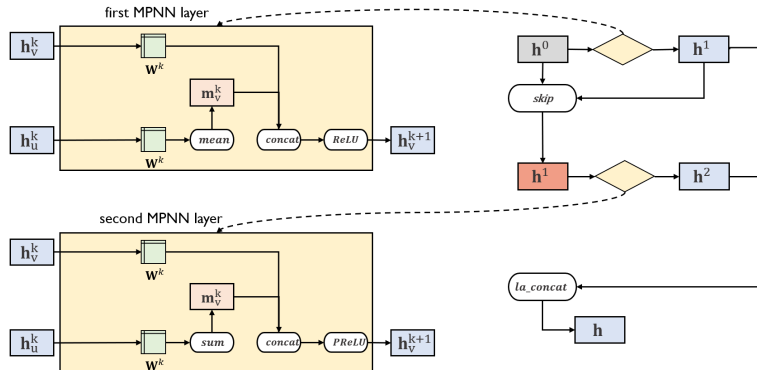


Figure 5: An example: GNN architecture searched by AutoGEL for the NC task on PubMed.

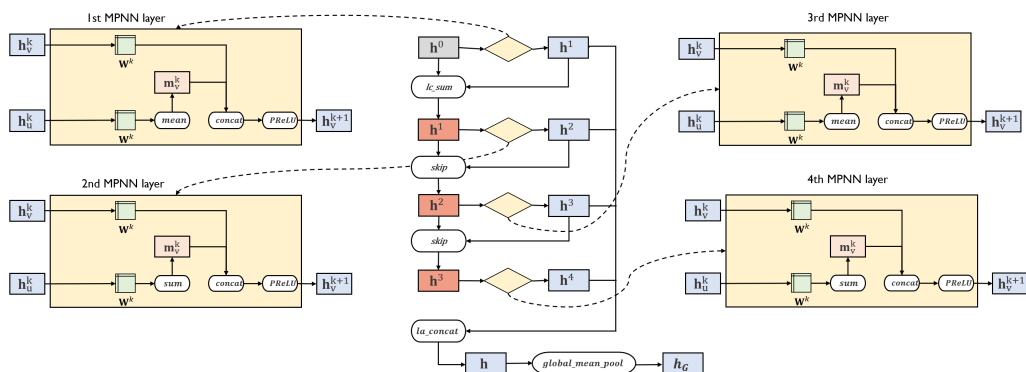


Figure 6: An example: GNN architecture searched by AutoGEL for the GC task on PROTEINS

resulting in performance degradation. Moreover, it is also discussed in [Zhang and Chen, 2018] that for subgraph-based LP approaches on homogeneous graphs adopted by AutoGEL, 2-hop enclosing subgraphs already contain rich information required for the prediction, therefore  $L > 2$  should not be very necessary.

Specifically, for the LP task on KG scenario, we empirically observe that the composition operator  $\phi(\mathbf{h}_u, \mathbf{h}_e)$  (see Sec. 3.1) should be one of the most critical components. This operator determines the way how to compose the neighborhood embedding  $\mathbf{h}_u$  and edge embedding  $\mathbf{h}_e$  to generate the message for the center node  $v$ . Actually, the composition operator  $\phi$  incorporates the scoring function design in past KG embedding models, such as subtraction for geometric models and multiplication for bilinear models. From experiments, we observed that  $\phi$  is data-dependent. *corr* is more preferred for the FB15k-237 dataset, and simpler *mult* is prone to get better results for the WN18RR dataset. Using others  $\phi$  for these data sets would lead to significantly different performance based on the empirical study.

For the NC task (see Fig. 5), pooling operator  $R(\cdot)$  is removed from the search space, and we set  $L = 2$  for all three citation datasets, since we observe performance degradation with larger  $L$  on those datasets.

For the GC task (see Fig.6), we empirically observe that AutoGEL prefers deeper GNN architectures compared to the LP and NC tasks. One potential reason is that, citation datasets adopted for the NC task are similar to “small world” networks [Barthélemy and Amaral, 2011] where each node can reach the entire graph within just a few hops. But the data sets for the GC task represent graph structures, such as molecules, where deeper architectures might be beneficial to increase effective receptive field. Besides, while the NC task mainly relies on local neighborhood (short-range) information, the GC task may require long-range information to capture certain graph properties that are essential to the prediction, such as chemical properties of molecules [Matlock et al., 2019], and graph moments [Dehmamy et al., 2019]. Thus deeper GNN architectures are more desired.

Table 9: Average AUC (with standard deviation) for LP task on homogeneous graphs

Type	Model	NS	Power	Router	C.ele	USAir	Yeast	PB
Heuristic	CN	94.42±0.95	58.80±0.88	56.43±0.52	85.13±1.61	93.80±1.22	89.37±0.61	92.04±0.35
	RA	94.45±0.93	58.79±0.88	56.43±0.51	87.49±1.41	95.77±0.92	89.45±0.62	92.46±0.37
	Katz	94.85±1.10	65.39±1.59	38.62±1.35	86.34±1.89	92.88±1.42	92.24±0.61	92.92±0.35
Latent	SPC	89.94±2.39	91.78±0.61	68.79±2.42	51.90±2.57	74.22±3.11	93.25±0.40	83.96±0.86
	LINE	80.63±1.90	55.63±1.47	67.15±2.10	69.21±3.14	81.47±10.71	87.45±3.33	76.95±2.76
	N2V	91.52±1.28	76.22±0.92	65.46±0.86	84.11±1.27	91.44±1.78	93.67±0.46	85.79±0.78
GLP	VGAE	94.04±1.64	71.20±1.65	61.51±1.22	81.80±2.18	89.28±1.99	93.88±0.21	90.70±0.53
	PGNN	94.88±0.77	-	-	78.20±0.33	-	-	89.72±0.32
	SEAL	98.85±0.47	87.61±1.57	96.38±1.45	90.30±1.35	96.62±0.72	97.91±0.52	94.72±0.46
	DE-GNN	99.09±0.79	96.68±0.29	98.69±0.17	89.37±0.17	98.04±0.66	98.59±0.26	94.95±0.37
AutoGNN	AutoGEL	<b>99.89±0.06</b>	<b>98.00±0.21</b>	<b>99.08±0.28</b>	<b>92.90±1.02</b>	<b>98.49±0.45</b>	<b>99.24±0.10</b>	<b>97.27±0.15</b>
	AutoGEL-intra	99.85±0.06	97.65±0.21	98.92±0.23	92.36±1.13	98.29±0.49	99.18±0.09	97.16±0.13
	AutoGEL-diff	99.58±0.17	97.05±0.19	98.92±0.27	90.38±0.64	97.89±0.69	98.90±0.10	96.12±0.21
	AutoGEL-\delta	99.85±0.06	97.65±0.20	98.98±0.23	92.58±1.14	98.33±0.39	99.14±0.09	97.23±0.07
	AutoGEL-darts	99.85±0.06	97.31±0.09	98.87±0.23	91.98±0.77	97.98±0.42	99.02±0.13	95.84±0.29

Table 10: MRR and Hits@N for LP task on knowledge graphs

Type	Model	FB15k-237				WN18RR			
		MRR	Hits@10	Hits@3	Hits@1	MRR	Hits@10	Hits@3	Hits@1
Geometric	TransE	.294	.465	-	-	.226	.501	-	-
	RotatE	.338	.533	.375	.241	<u>.476</u>	<b>.571</b>	<u>.492</u>	.428
Bilinear	DisMult	.241	.419	.263	.155	.430	.490	.440	.390
	CompLex	.247	.428	.275	.158	.440	.510	.460	.410
NN-based	ConvKB	.243	.421	.371	.155	.249	.524	.417	.057
	ConvE	.325	.501	.356	.237	.430	.520	.440	.400
	ConvR	.350	.528	.385	.261	.475	.537	.489	<u>.443</u>
	HyperER	.341	.520	.376	.252	.465	.522	.477	.436
GLP	R-GCN	.248	.417	-	.151	-	-	-	-
	SACN	.350	<b>.540</b>	<u>.390</u>	.260	.470	.540	.480	.430
	VR-GCN	.248	.432	.272	.159	-	-	-	-
	CompGCN	.355	.535	<u>.390</u>	.264	<b>.479</b>	.546	<b>.494</b>	<u>.443</u>
AutoGNN	AutoGEL	<b>.357</b>	<u>.538</u>	<b>.391</b>	<b>.266</b>	<b>.479</b>	<u>.549</u>	<u>.492</u>	<b>.444</b>
	AutoGEL-\lambda	.355	.533	.389	<u>.265</u>	.470	.532	.486	.434
	AutoGEL-darts	.356	<u>.538</u>	<b>.391</b>	<u>.265</u>	.472	.544	.485	.434
	AutoGEL-\h_e	.355	.531	.389	<u>.265</u>	.454	.540	.483	.402

### A.3 Ablation Study

Apart from the main experiment results shown in Sec. 4, we also conduct several ablation studies to investigate the influence of different components in AutoGEL and provide additional experiments in this section.

1) *Impact of Inter-level Design*: AutoGEL provides various design dimensions from both intra-level (see Sec.3.1.1) as well as inter-level (see Sec.3.1.2). To study the effect of the proposed inter-level designs, we set a variant, i.e., AutoGEL-intra, where inter-level design dimensions are removed from the search space, and we only conduct operator search from intra-level. As shown in Tab. 9 and Tab. 11, AutoGEL-intra achieves competitive performance compared with manually-designed GNN baselines, which illustrates the powerfulness of AutoGEL’s intra-level designs. But AutoGEL brings more performance gains over AutoGEL-intra by searching inter-level operators. Note that the number of layers  $L$  for the LP task on KG is usually 1 (see Appendix A.2), thus there are no results of AutoGEL-intra in Tab. 10.

2) *Impact of Pooling Operator*: In this paper, we provide pooling operation candidates  $R(\cdot) \in \{sum, mean, max\}$  for the LP task on homogeneous graphs. As discussed in Sec. 3.1.3, DEGNN [Li et al., 2020] utilizes the difference-pooling as  $R(\cdot)$ . Here we set a variant, i.e., AutoGEL-diff, where we remove the proposed pooling candidates from the search space and fix the difference-pooling instead. As shown in Tab. 9, the fixed difference-pooling method leads to the significant performance degradation, illustrating the strength of AutoGEL’s pooling design.

Table 11: Average accuracy (%) for node classification and graph classification

Type	Model	Node Classification			Graph Classification			
		Cora	CiteSeer	Pubmed	IMDB-B	IMDB-M	MUTAG	PROTEINS
Manual GNNs	PATCHYSAN	-	-	-	71.00	45.20	92.60	75.90
	DGCNN	-	-	-	70.00	47.80	85.80	75.50
	GCN	88.11	76.66	88.58	74.00	51.90	85.60	76.00
	GraphSAGE	87.41	75.99	88.34	72.30	50.90	85.10	75.90
	GAT	87.19	75.18	85.73	-	-	-	-
	GIN	86.00	73.40	87.99	75.10	52.30	89.40	76.20
AutoGNN	GraphNAS	88.40	77.62	88.96	-	-	-	-
	SANE	89.26	<b>78.59</b>	<b>90.47</b>	-	-	-	-
	You et al. [2020]	88.50	74.90	-	-	47.80	-	73.90
	AutoGEL	<b>89.66</b>	<u>77.66</u>	<u>90.00</u>	<b>81.20</b>	<b>56.80</b>	<b>96.14</b>	<b>82.68</b>
	AutoGEL-intra	88.93	76.33	89.73	<u>77.62</u>	<u>55.58</u>	95.98	77.96
	AutoGEL- $\delta$	88.88	76.55	89.96	77.44	53.88	93.75	79.3
AutoGEL-darts	89.00	77.49	89.85	76.69	47.42	<u>96.05</u>	<u>80.08</u>	

Table 12: Search time (clock time in seconds) comparison on the node classification (NC) task and graph classification (GC) task

	Node Classification			Graph Classification			
	Cora	CiteSeer	PubMed	IMDB-B	IMDB-M	MUTAG	PROTEINS
AutoGEL	12	16	19	58	90	2.4	56
AutoGEL-darts	15	31	97	122	138	3.8	95

Table 13: Search time (clock time in hours) comparison on the LP task

	NS	Power	Router	C.ele	USAir	Yeast	PB	FB15k-237	WN18RR
AutoGEL	0.5	2.6	3.4	1.4	1.3	4.0	14.4	18.1	13.1
AutoGEL-darts	1.0	2.7	3.4	1.5	1.4	6.0	14.7	18.3	13.7

3) *Impact of Separate Weight Transformation Matrices:* AutoGEL provide novel linear transformation approaches, i.e., we assign neighborhood-type specific matrices  $\mathbf{W}_{\delta(u)}^k$  as special attention mechanism for homogeneous graphs, and edge-aware filters  $\mathbf{W}_{\lambda(e)}^k$  to incorporate information from different directions for heterogeneous graphs (see Sec. 3.1.1). To study the impact of such designs, we provide two variants, i.e., AutoGEL- $\delta$  (see Tab. 9 and 11) and AutoGEL- $\lambda$  (see Tab. 10), where  $\mathbf{W}_{\delta(u)}^k$  and  $\mathbf{W}_{\lambda(e)}^k$  are simply replaced by a single  $\mathbf{W}^k$ . Compared with these two variants, AutoGEL achieves better performance cross different graph tasks and datasets.

4) *Impact of Edge Embedding:* To show the effectiveness of edge embedding  $\mathbf{h}_e$  on the LP task, we set another variant, i.e., AutoGEL- $\mathbf{h}_e$ , by removing  $\mathbf{h}_e$  from AutoGEL’s MPNN and simply replace  $\phi(\mathbf{h}_u^k, \mathbf{h}_e^k)$  with  $\mathbf{h}_u^k$  in (8). Experiment results are shown in Tab. 10. Performance degradation is observed for the AutoGEL- $\mathbf{h}_e$ , especially on the WN18RR dataset, indicating that  $\mathbf{h}_e$  is indeed a critical design.

5) *Impact of Stochastic Differentiable Search Algorithm:* As discussed in Sec.3.2, AutoGEL adopts stochastic differentiable search algorithm in SNAS to perform more effective and efficient architecture search. To show its superiority, we also try the deterministic differentiable search algorithm DARTS for AutoGEL, denoted as AutoGEL-darts. Tab. 9, Tab. 10, and Tab. 11 empirically show the consistent superior performance of the AutoGEL compared with AutoGEL-darts variant cross node/edge/graph level tasks, indicating the effectiveness of AutoGEL’s search algorithm. Besides, we further show that the search cost of AutoGEL is also lower than its AutoGEL-darts variant (see Tab. 12, and Tab. 13).

Table 14: Running time (clock time in hours) of AutoGEL and several baselines for the LP task

Type	Model	HGs							KGs	
		NS	Power	Router	C.ele	USAir	Yeast	PB	FB15k-237	WN18RR
GLP for HG	DE-GNN	0.1	1.0	1.2	0.2	0.3	2.0	4.7	-	-
Bilinear for KG	DistMult	-	-	-	-	-	-	-	2.6	0.4
NN for KG	ConvE	-	-	-	-	-	-	-	26.0	10.2
GLP for KG	CompGCN	-	-	-	-	-	-	-	16.1	7.8
Ours	AutoGEL (search)	0.5	2.6	3.4	1.4	1.3	4.0	14.4	18.1	13.1
	AutoGEL (training)	0.3	0.5	0.7	0.4	0.4	1.5	4.8	13.1	7.3

#### A.4 Search Efficiency

As mentioned in Sec. 4.2, we found that existing GLP modes generally require more computational resources in practice. Thus, we try to reduce the search cost in the proposed AutoGEL. Tab. 14 reports the running time (hours) of AutoGEL and several other representative baselines for the LP task on the homogenous graph (HG) and knowledge graph (KG).

From Tab. 14, we can observe that: On the LP task on HGs (NA, Power, Router, C.ele, USAir, Yeast, and PB), AutoGEL runs quite fast, which substantially eases the difficulty of using AutoGEL. Besides, AutoGEL achieves more significant performance boost in this scenario (see Tab. 2). On the LP task on KGs (FB15K-237, WN18RR), DistMult [Yang et al., 2014] is a representative of bilinear models that run much faster among all KGE models. Although AutoGEL is slower than DistMult, its computational cost is very close with classic neural networks (NNs) for KG ConvE [Dettmers et al., 2018] and GLP model CompGCN [Vashishth et al., 2019]. Then recalling Tab. 3, AutoGEL well balances between search cost and effectiveness.